# Mobile LiDAR Data and Imagery for Digital Twin Generation

Shabnam Jabari [1], Faith Nayko [2] Derek Lichti[2], Scott Morrison[1], Scott Whitters[1], Logan Kennedy[1], Mark Masry[3]

[1] UNB, Geodesy and Geomatics Engineering, (sh.jabari, scott.morrison, swhitter, lkenned4)@unb.ca
[2] University of Calgary, Geomatics Engineering, (faith.nayko, ddlichti)@ucalgary.ca
[3] Modelar, mark@modelar.ai

**Keywords:** iPhone LiDAR, Digital Twins, Mapping accuracy, Constrained Bundle Adjustment, Ultrasonic Positioning System.

**Abstract**

Low-cost sensor solutions such as smartphones provide a great opportunity for democratization of mapping among different communities including those working in digital twin application areas. Smartphone acquired imagery and/or built-in LiDAR sensors provide relatively dense point clouds with limited accuracy especially in the absence of GNSS. This type of scanning tool can provide linear measurements in an inexpensive way and can be used with minimal operator training. In this study, we provide two solutions for improving the accuracy of the final point clouds produced by iPhone-based LiDAR and images. One solution utilizes length observations as constraints in the network. The other solution incorporates loosely coupled perspective centre (PC) positions obtained by ultrasonic ranging into a photogrammetric bundle adjustment. The test results show that inclusion of the length observations in the solution improves the relative accuracy of the point cloud for applications such as culvert mapping where absolute accuracy is not of high necessity. In the indoor mapping case, the relative point cloud accuracy for the solutions without and with the PC observations is approximately the same. However, image alignment success and computation time are significantly improved by including the PC observations. Moreover, the inclusion of PC observations provided better compensation of systematic image point errors.

## 1. Introduction

The growing importance of new mobile devices with LiDAR sensors for reality capture data collection has been documented (Tavani et al., 2022). The use of these low-cost and ubiquitous devices lowers entry barriers to the ever-growing reality capture market (Vogt et al., 2021). However, it is well-studied in the literature that such mapping solutions have limited accuracy. There are other studies in the literature that address improving spatial accuracy of such sensors for different mapping applications. In one of our early studies, Chase et. al. (2022) tested the iPhone-13 Pro LiDAR using Modelar's scanning application with a network of GCPs. The study was conducted in a surveying lab at the University of New Brunswick, which contains a high-precision control network. Checkerboard targets were established at different heights and positions to ensure varied depths and exclude correlated errors. The performance was compared to a Trimble TX5 Terrestrial Laser Scanner (TLS) in a controlled environment. The absolute and relative accuracies were assessed by comparing test point coordinates and distances measured respectively, using a Trimble S9 total station as a reference. Results indicate that the iPhone-13 Pro achieved absolute accuracies of ±3 cm horizontally and ±7 mm vertically, and relative accuracies of ±3 cm.

Other studies constrain the network with auxiliary observations. There exist several recent reports on the performance testing of these devices' LiDAR sensors in support of various capture applications such as earth sciences (Vogt et al., 2021), forestry (Gollob et al., 2021), forensics (Kottner et al., 2023), indoor mapping (Teo, 2015) and cultural heritage recording (Teppati Losè et al., 2022; Vacca, 2023). Data quality is reported to be greatly influenced by the choice of the software app used to create the point cloud and many artefacts (Lichti et al., 2005) contaminate the data. The need for rigorous geometric modelling of the interior geometry of these devices and development of geometric calibration procedures has been identified has a high priority for high-quality metric reality capture. Moreover, the use of independent observations to improve the quality of point clouds produced from mobile devices requires additional investigation.

In this submission, we introduce two studies relevant to iPhone-based mapping solutions from two research labs in Canada: Advanced Spatial Intelligence Lab (ASIL) at University of New Brunswick (UNB) and Geospatial Vision Meteorology (GVM) Lab at University of Calgary (UC). One study focuses on constrained bundle adjustment using length observations in an indoor environment. The other study utilizes ultrasonic position observations as auxiliary data.

## 2. Mapping Solutions

### 2.1 Length-based Constrained Network

The accuracy of mobile LiDAR scans is compromised by tracking loss and positional drift, especially in indoor environments with minimal features, such as culverts. This part of the solution, tested in ASIL at UNB, aims to develop a methodology that mitigates these errors, enhancing the utility of mobile Camera and LiDAR for culvert assessments. In this study, while the absolute accuracy of the final 3D model is not the primary focus, ensuring high relative accuracy is crucial for effective culvert maintenance. For data collection using the iPhone LiDAR and RGB images the Modelar app was used.

Linear constraints are independent distance measurements collected in the field. When implemented into bundle adjustment as constraints, they prevent the network from bending, twisting or scaling and, thus, improve the accuracy of the final 3D model. Figure 1 (right) represents one of the constrained networks tested. Pix4D was chosen as the software for processing due to its ability to implement constraints into its bundle adjustment. Different configurations of these constraints were tested, which will be discussed in a later section. The model created in this part of the study is called the Length-based Constrained Bundle Adjustment (LCBA).

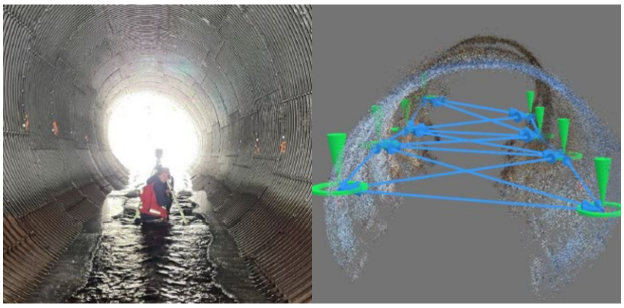

Figure 1: left: the culvert scanned in this study; right: Config. 3 for constrained lengths.

### 2.2 Perspective Centre Position Aided Mapping Network

Generating 3D indoor models can pose challenges due to the difficulty of accurately orienting photogrammetry sensors in the absence of GNSS signals, which are essential for precise positioning in outdoor environments. Traditional photogrammetric methods rely on ground control points established through conventional survey methods, which, while effective, are costly, labour-intensive, and limit scalability. Simultaneous localisation and mapping (SLAM) solutions offer an alternative by integrating sensor data to build 3D maps while tracking the sensor's position in real time. However, SLAM approaches often struggle in feature-poor or highly similar environments, where a lack of distinct visual or geometric landmarks can lead to localization errors (Xiang et al., 2024). Additionally, SLAM is widely used in real-time applications, but its effectiveness is often limited by its high computational demands, which can introduce latency and reduce performance in systems with constrained processing power and memory (Semenova et al., 2024). Addressing these challenges is essential for facilitating the widespread adoption of indoor digital twin technology, especially in applications that demand frequent updates and high adaptability.

ZeroKey's Quantum RTLS (real-time location system) presents a potential solution for providing real-time position and estimates for photogrammetry sensors. This system employs a hybrid approach that combines ultrasonic time-of-flight (TOF) ranging with electromagnetic wave synchronization to achieve sub-millimetre positioning precision (Leskiw et al., 2020). Unlike radio frequency-based indoor positioning systems such as ultra-wideband and Bluetooth, which suffer from limited accuracy due to signal interference and multipath effects (Singh et al., 2024), ZeroKey's system utilizes ultrasonic waves for its range measurements. Because sound waves travel significantly slower than radio waves, the Quantum RTLS can achieve finer distance resolution, contributing to high-quality range measurements. To ensure synchronization, the system leverages electromagnetic signals as a precise time reference, mitigating clock drift and latency issues that typically affect TOF-based methods. The ZeroKey system comprises a set of synchronized anchor nodes mounted throughout measurement volume site and a mobile node.

The high-accuracy positioning provided by the Quantum RTLS system has the potential to eliminate the need for traditional ground control points—much like GPS did for aerotriangulation in the early 1990s. GPS-assisted photogrammetry revolutionized aerial mapping by reducing the number of ground control points (GCPs) required to control error propagation in a block. The inclusion of perspective centre (PC) observations in the block served to control error propagation. Thus, instead of a dense network of GCPs, as little as four were needed, provided certain conditions were met (Ackermann, 1992). Moreover, the inclusion of the PC position observations will accurately scale the photogrammetrically produced point cloud. Point clouds generated from structure from motion processing pipelines are often arbitrarily scaled. External information is needed to provide metric scale for the bundle network, which can be provided by accurate PC observations. Our vision is to integrate Quantum RTLS observations of the mobile device into the bundle adjustment framework. This paper investigates the implications of this integration for image-based networks. Future research will explore its impact on LIDAR-based networks.

## 3. Experiment Descriptions

### 3.1 Length-based Constrained Network

The first solution was implemented at a culvert site in New Brunswick, Canada (named L458) and was chosen for its challenging scanning conditions. The length of the culvert is around 60m with the diameter of around 5m. Data collection involved three main stages: target placement, mobile LiDAR scanning using the Modelar application (which uses a SLAM solution for 3D mapping), and ground truth data collection using a Trimble TX5 TLS and a total station. Reflective targets were placed at ~2.5 m intervals within the culvert, and their coordinates were recorded using the total station. Mobile LiDAR scans were performed in sections to limit error accumulation; and, as constraints, distance measurements between targets were taken using a Leica Disto D2 laser distance measurement tool. Three distinct datasets were processed: the ground truth TLS data, the Modelar scan data, and the LCBA model. The TLS data were processed using Faro Scene, while the Modelar data was processed using its proprietary software. The LCBA model was processed in Pix4D Mapper, incorporating linear constraints derived from the distance measurements. This approach aimed to correct positional drift and improve the overall accuracy of the mobile LiDAR scans.

Modelar uses Apple's SLAM framework to estimate the device positions relative to a starting position. For this experiment no additional corrections were performed to improve these estimates; the results are therefore determined entirely by the quality of the underlying SLAM system. The accuracy of the Modelar scans was evaluated by comparing them to the ground truth TLS data using CloudCompare software. The analysis focused on the mean distance and deviations in the X, Y, and Z directions. For the ease in data collection the culvert was divided into 3 sections and the resulting point clouds were registered together to make the full culvert 3D model. For testing the configuration of the length-based constrained, three configurations of Across_diagonal (Config. 1), Across_short-length (Config. 2), and Across_diagnal_short-length (Config. 3), were tested to determine the optimal setup for improving scan accuracy (Figure 2).


https://doi.org/10.5194/isprs-archives-XLVIII-4-W15-2025-71-2025  

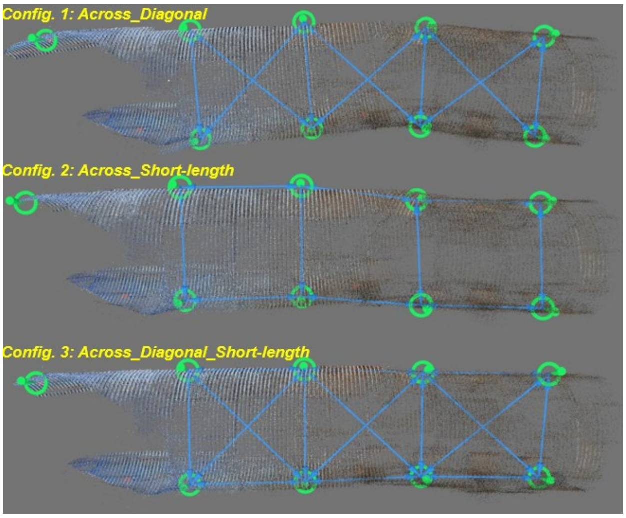


Figure 2: Different configuration of the linear constrained tested

### 3.2 Perspective Centre Position Aided Mapping Network

The second solution investigated was mobile phone imagery loosely coupled with an external positioning system tested in an indoor environment at the University of Calgary. A recently renovated and furnished kitchen and dining area (approximate dimensions of 8 m x 6 m x 3 m; Figure 3) was mapped with several sensors. An Apple iPhone 12 Pro mobile device was used to collect both images and LIDAR data. The primary (wide) camera of the phone, which has a sensor format is 4032 x 3024 pix, was used. The nominal physical focal length 4.2 mm, with a 35mm equivalent focal length of 26 mm. The aperture was set to f/1.6 for data capture. LiDAR data were captured with the Record3D app at 6 fps using the highest available resolution. Ten ZeroKey anchors were installed throughout the measurement volume, most of which (eight) were on the ceiling.

To tightly control the experiment conditions, the iPhone and the mobile ZeroKey were mounted in a smartphone rig (Figure 4) and set up on a tripod at a height of 1.5 m above the floor. Data were captured in two laps round the periphery of the room. The tripod stations were spaced to achieve 60-80% overlap between adjacent images. For the first lap, the camera faced the direction of travel, while for the second lap it faced inward. A total of 181 images stations were captured. A landscape format image and LiDAR data along with 30 s of ZeroKey position data were collected at each station. Terrestrial laser scanner data were collected as reference data to quantify the quality of point clouds derived from the iPhone sensor data. Six scans were captured from around the room with a Faro Focus 3D scanner. These data were finely registered in CloudCompare following coarse, manual registration.

Figure 3. University of Calgary indoor environment.

Photogrammetric data processing was performed using Agisoft MetaShape. Two processing cases were preformed: one that incorporated the Quantum RTLS camera PC positions as observations into the self-calibrating bundle adjustment; and one that did not. The self-calibration model included the principal distance, principal point, three radial lens distortion terms and two decentring lens distortion terms. Rolling shutter compensation was also included.

Recent quality assessment findings for the ZeroKey system (Nayko and Lichti, 2025) indicated sub-centimetre positional accuracy can be achieved. However, a more pessimistic value of 0.05 m for the PC positions' *a priori* standard deviation was required for the bundle adjustment. Some of the pertinent software settings common to both processing cases were exclusion of stationary tie points and moderate depth filtering for point cloud densification. The generated dense point clouds were registered by ICP to the laser scanner point cloud in CloudCompare using the same procedure of coarse manual alignment followed by fine registration.

Figure 4. Smartphone rig with Apple iPhone 12 Pro and ZeroKey Quantum RTLS mobile node (at upper left).

## 4. Experiment Results

This section reports the results of the two solutions that were compared against ground truth. Table 1 lists the accuracy metrics used in this study.

| Metric | Description |
|---|---|
| Mean Distance (MD) | The average absolute deviation between the test and reference (TLS) data. |
| Error in X, Y, Z Directions | The standard deviation (STD) between nearest points in certain direction |
| Confidence Interval (CI) | 99% considering normal distribution |
| Root mean square (RMS) | The square root of the mean squared distance between point clouds. |

Table 1: Accuracy assessment metrics used.

### 4.1 Length-based Constrained Network

A comprehensive evaluation using CloudCompare's analysis tools was conducted to assess the absolute accuracy of the Modelar point cloud and the effectiveness of the applied constraints in improving positional accuracy.

The analysis incorporated a quantitative comparison between the reference point cloud and the test point clouds, presented in histograms for the original Modelar scan (Figure 5) and the tested configurations (Figure 6). In these visualizations, blue tones indicate minimal deviations, while red tones highlight maximum discrepancies, providing a clear and intuitive representation of the data's reliability and the scanning method's overall performance. The horizontal axis shows the deviation between the two-point clouds (i.e., cloud-to-cloud distance: C2C), while the vertical axis represents the number of points.
The C2C error graph was generated by comparing the scan data to a full culvert model, which was assembled by visually aligning the three sections from the worst of the two available passes. This approach was intentional, designed to provide the team with a suboptimal reference model to highlight areas requiring correction. As a result, some of the observed errors likely reflect this intentionally degraded alignment and may not be representative of typical performance. Therefore, the error distribution should be interpreted with this context in mind. The intention was not to compare the individual sections to the full registered culvert model, but rather to demonstrate that, after registration, the sections achieved results comparable in accuracy and quality to the complete model.

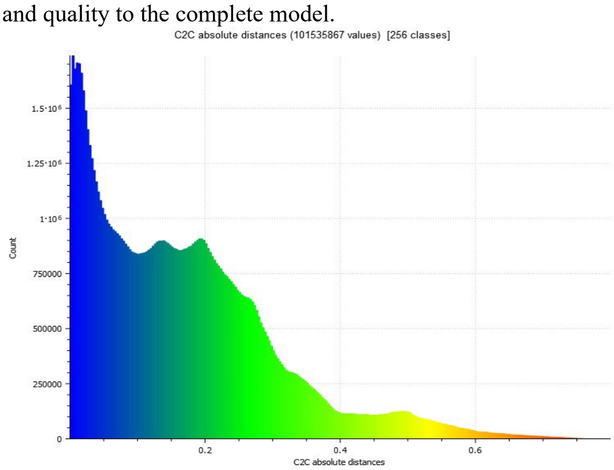


Figure 5: C2C distance of the Modelar raw point clouds with the reference point cloud

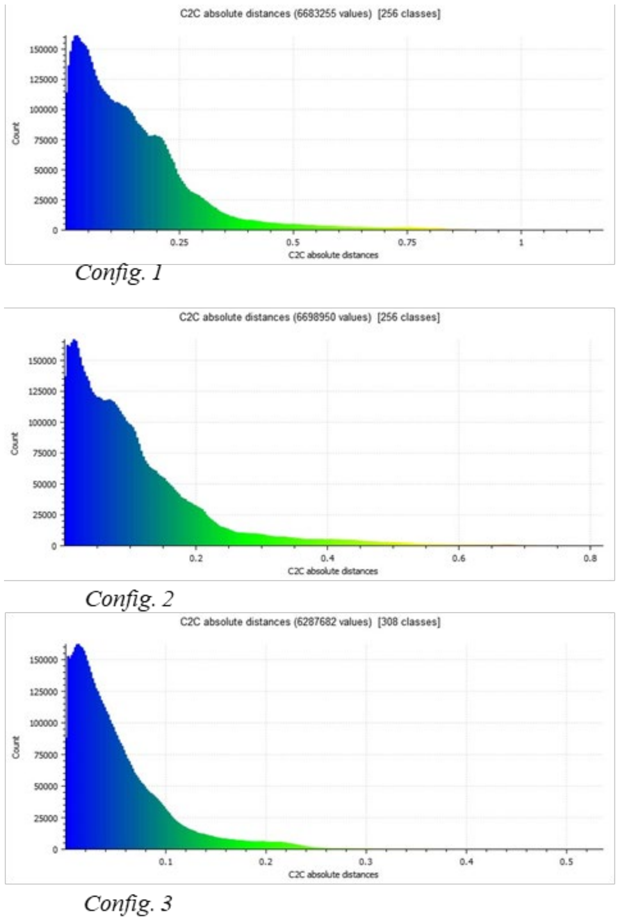


Figure 6: C2C distance of the test point clouds with the reference point cloud

Tables 2 and 3 compare the accuracy of different configurations to the original (Modelar SLAM) and registered point clouds. The LCBA Config.3 model showed significant improvements, with a mean distance error reduced to 5.8 cm, compared to 17.4 cm for the unconstrained Modelar scans. The integration of linear constraints into the mobile LiDAR scanning workflow resulted in an improvement in relative scan accuracy.

| **Model** | | | **MD (m)** | **STD (m)** | | |
|---|---|---|---|---|---|---|
| | | | | **X** | **Y** | **Z** |
| SLAM | Full | Modelar | 0.065 | 0.185 | 0.099 | 0.168 |
| LCBA | Sec. 3 | Config 1 | 0.064 | 0.147 | 0.113 | 0.165 |
| | | Config 2 | 0.058 | 0.089 | 0.099 | 0.149 |
| | | Config 3 | **0.028** | **0.047** | **0.046** | **0.072** |
| | Full | Registered | 0.031 | 0.059 | 0.053 | 0.08 |

Table 3: The MD and STD results of the first solution in this study.

| Model | | | CI (m) | | |
|---|---|---|---|---|---|
| | | | X | Y | Z |
| SLAM | Full | Modelar | 0.168 | 0.478 | 0.255 |
| LCBA | Sec. 3 | Config 1 | 0.165 | 0.379 | 0.291 |
| | | Config 2 | 0.149 | 0.229 | 0.255 |
| | | Config 3 | **0.072** | **0.121** | **0.118** |
| | Full | Registered | 0.08 | 0.153 | 0.136 |

Table 4: The CI results of the first solution in this study.

### 4.2 Perspective Centre Position Aided Mapping Network

Pertinent results from the bundle adjustments are first analysed. The image point residuals indicate the quality of the observations' fit to the collinearity model. The overall root mean square (RMS) of the residuals (reprojection error) for the cases without PC observations and with the ZeroKey PC observations were 0.71 pix and 1.21 pix, respectively. The inflation of the latter case can be expected due to the introduction of another set of observations. However, the compensation of systematic errors appears to be superior for the case with PC observations. Figure 7 shows the residual vectors for the adjustment without positions. Evidence of unmodelled radial distortion is visible, whereas the residuals from the case with PC observations (Figure 8) exhibit random behaviour.

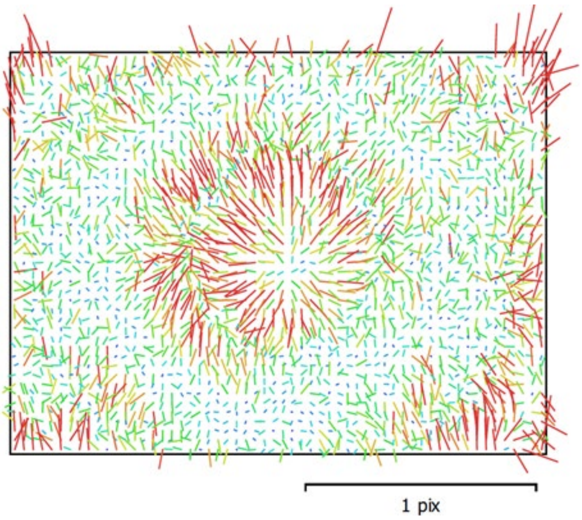


Figure 7: Image point residuals from the self-calibration without PC position observations.

The RMS of differences between the photogrammetrically generated point clouds and the laser scanner data were 0.039 m and 0.040 m, respectively. Thus, based on model fit and overall 3D reconstruction accuracy, the introduction of PC observations is effectively the same as the case without any prior positional information.

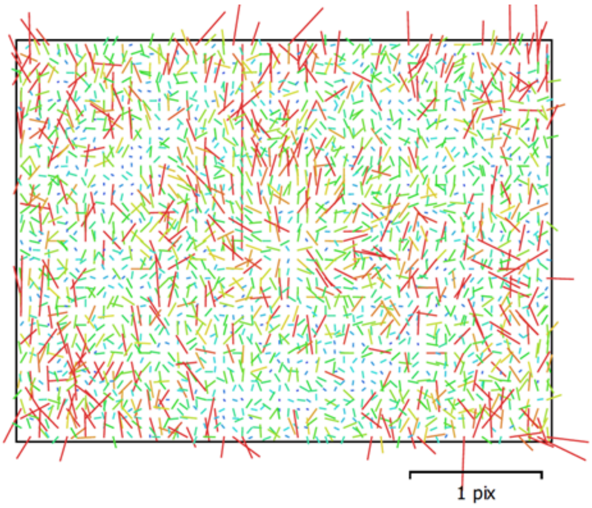


Figure 8: Image point residuals from the self-calibration with PC position observations.

| With PC obs? | With guided image matching? | # of images aligned (out of 181) | Processing time to align images (s) |
|---|---|---|---|
| No | No | 181 | 124 |
| No | Yes | 115 | 11 |
| Yes | Yes | 181 | 55 |

Table 4. Photogrammetric alignment and processing time.

Reduction in photogrammetric processing time and improved alignment success were found to be advantages of incorporating the PC observations. Table 4 provides a summary for three different cases: with PC observations and guided image matching; and two cases without PC observations, with and without guided image matching. Guided image matching can increase the number of key points extracted from each image without significantly increasing processing time (Agisoft LLC, 2024). Without PC positions, image alignment is successful but takes much longer without the guided image matching option. Although processing time for image alignment is reduced by an order of magnitude, 36% of the images could not be aligned. Inclusion of the *a priori* PC positions allows all images in the network to be aligned, although the processing time compared to the case without the extra observations increases by 5x. However, this is an improvement in processing time over the base case by more than 2x. Thus, including PC observations is beneficial to the success of image alignment and can improve alignment time.

## 4. Conclusions

The solution regarding the optimized constraint configuration across the full culvert demonstrated a marked improvement in the accuracy of the LCBA model. The final mean error of Modeler SLAM was reduced to 5.8cm, with the X direction showing the least deviation and the Y and Z directions exhibiting slightly higher errors, likely due to the alignment of targets along a single plane. Among the tested configurations, Config. 3 proved to be the most effective, achieving an average distance of 5.3 cm and confirming the importance of incorporating measurements along the culvert's length in both cross and alongside directions.

In the indoor mapping case, the relative point cloud accuracy for the solutions without and with the PC observations was approximately the same, 3.9 cm and 4.0 cm, respectively. However, image alignment success and computation time are significantly improved by including the PC observations. Moreover, the inclusion of PC observations provided better compensation of systematic image point errors.

In this study, we proposed two solutions for 3D mapping, which serves as the foundation for digital twin applications. The overall conclusion is that if lightweight SLAM algorithms, such as the Modelar iPhone app, are supplemented with external auxiliary observations for Exterior Orientation Parameters (EOP) from systems like ZeroKey, the accuracy can be significantly improved. In cases where the EOP auxiliary measurements are not available, length constraints can still be valuable for generating scaled 3D models. When absolute positioning is required, georeferencing becomes essential.

**Acknowledgements**

Funding for this research has been provided by the Natural Sciences and Engineering Research Council of Canada (RGPIN-2024-03793 and RGPIN-2020-04698). The authors gratefully acknowledge the support of ZeroKey for providing access to their positioning system for experimental use.

**References**

Ackerman, F., 1992. Kinematic GPS control for photogrammetry. *Photogrammetric Record*, 14(80): 261–276.

Agisoft LLC, 2024. Agisoft Metashape User Manual: Professional Edition, Version 2.1.

Chase, P. P. C., Clarke, K. H., Hawkes, A. J., Jabari, S., & Jakus, J. S. (2022). Apple iPhone 13 Pro LiDAR accuracy assessment for engineering applications. *2022: The Digital Reality of Tomorrow*, 1–10.

Gollob, C., Ritter, T., Kraßnitzer, R., Tockner, A., Nothdurft, A., 2021. Measurement of Forest Inventory Parameters with Apple iPad Pro and Integrated LiDAR Technology. Remote Sensing 13, 3129. https://doi.org/10.3390/rs13163129

Kottner, S., Thali, M.J., Gascho, D., 2023. Using the iPhone's LiDAR technology to capture 3D forensic data at crime and crash scenes. Forensic Imaging 32, 200535. https://doi.org/10.1016/j.fri.2023.200535

Leskiw, C., Gao, G., Lowe, M., 2020. ZeroKey's Smart Space indoor positioning system [White paper]. ZeroKey Inc. Retrieved March 22, 2023 from https://zerokey.com/

Lichti, D.D., Gordon, S.J., Tipdecho, T., 2005. Error Models and Propagation in Directly Georeferenced Terrestrial Laser Scanner Networks. Journal of Surveying Engineering 131, 135–142. https://doi.org/doi.org/10.1061/(ASCE)0733-9453(2005)131:4(135)

Nayko, F., Lichti, D.D. 2025. Indoor digital twins: Evaluating smartphone models oriented with ultrasonic positioning against TLS. Accepted for publication in 46th Canadian Symposium on Remote Sensing, Lethbridge, Canada, 16-19 June 2025.

Semenova, S., Ko, S., Liu, Y. D., Ziarek, L., & Dantu, K. (2024). A Comprehensive Study of Systems Challenges in Visual Simultaneous Localization and Mapping Systems. *ACM Trans. Embed. Comput. Syst.*, *24*(1), 2:1-2:31. https://doi.org/10.1145/3677317

Singh, J., Tyagi, N., Singh, S., Ali, F., & Kwak, D. (2024). A Systematic Review of Contemporary Indoor Positioning Systems: Taxonomy, Techniques, and Algorithms. *IEEE Internet of Things Journal*, *11*(21), 34717–34733. IEEE Internet of Things Journal. https://doi.org/10.1109/JIOT.2024.3416255

Tavani, S., Billi, A., Corradetti, A., Mercuri, M., Bosman, A., Cuffaro, M., Seers, T., Carminati, E., 2022. Smartphone assisted fieldwork: Towards the digital transition of geoscience fieldwork using LiDAR-equipped iPhones. Earth-Science Reviews 227, 103969. https://doi.org/10.1016/j.earscirev.2022.103969

Teo, T., 2015. VIDEO-BASED POINT CLOUD GENERATION USING MULTIPLE ACTION CAMERAS. Int. Arch. Photogramm. Remote Sens. Spatial Inf. Sci. XL-4/W5, 55–60. https://doi.org/10.5194/isprsarchives-XL-4-W5-55-2015

Teppati Losè, L., Spreafico, A., Chiabrando, F., Giulio Tonolo, F., 2022. Apple LiDAR Sensor for 3D Surveying: Tests and Results in the Cultural Heritage Domain. Remote Sensing 14, 4157. https://doi.org/10.3390/rs14174157

Vacca, G., 2023. 3D Survey with Apple LiDAR Sensor—Test and Assessment for Architectural and Cultural Heritage. Heritage 6, 1476–1501. https://doi.org/10.3390/heritage6020080

Vogt, M., Rips, A., Emmelmann, C., 2021. Comparison of iPad Pro®'s LiDAR and TrueDepth Capabilities with an Industrial 3D Scanning Solution. Technologies 9, 13.

Xiang, Z., Guo, J., Meng, J., Meng, X., Li, Y., Kim, J., Wang, S., Lu, B., & Chen, Y. (2024). Accurate localization of indoor high similarity scenes using visual slam combined with loop closure detection algorithm. *PLOS ONE*, *19*(12), e0312358. https://doi.org/10.1371/journal.pone.0312358